<u>Journal of Advanced Sciences and Engineering Technologies</u> (2024).(7)1:54-62 https://doi.org/10.-32441/jaset.07.01.04



Journal of Advanced Sciences and Engineering Technologies
https://isnra.net/ojs/index.php/jaset/index/



Radiation Properties of Two Elements Microstrip Antenna Array at Microwave Frequencies

Ayman Al-Sawalha

Physics Department, Faculty of Science, Jerash University, Jerash 31982, Jordan

* E-mail :draymansawalha@gmail.com

Keywords:

active antenna, microstrip antenna, beam scanning, and active patch array

ARTICLE INFO

Article history:

Received: 03 January 2024
Received in revised form: 28 March 2024
Accepted: 02 April 2024
Available online: 08 May 2024

©2022 THIS IS AN OPEN-ACCESS ARTICLE UNDER THE CC BY LICENSE http://creativecommons.org/licenses/by/4.0/





Citation:

Ayman, A.-S. (2024). Radiation Properties of Two Elements Microstrip Antenna Array at Microwave Frequencies. Journal of Advanced Sciences and Engineering Technologies, 7(1), 55–65. https://doi.org/10.32441/jaset.07.01.04

ABSTRACT

One of the critical challenges in developing radio communicat

systems is the creation of tiny solid-state radiation sources, particula in the microwave and millimeter range; an antenna serves as the effici interface between electronic circuits and the external environme making it a crucial element in the growing trend of using high frequence in contemporary wireless communications. The card actively contribu to developing several subsystems for an active monolithic Phased Ar Antenna, which utilizes solutions in space technology and anter technologies operating at frequencies of around 30 GHz and 28 Gl such as Local Multipoint Distribution (LMDS). This document primar focuses on the study method and the two components of active pa arrays. The radiation models were computed utilizing the cavity pl model, the Simple Green model, and the rigorous commerc Electromagnetic Simulator. The active rectangular patches with the Ga diode were reconfigured and assembled into arrays in the E-plane and plane. The calculated and measured findings for both active arrays ha proved the potential for beam scanning. All three models have accurat projected radiation levels across a wide range of steering controls. ensure stable operation, a thin dielectric layer was positioned in front the H plane of the array. The impact of the dielectric layer on the ev and odd modes of the array has been demonstrated.

1. Introduction

As the number of users grows, the available frequency allotment decreases because of the limited channel capacity. The maximum number of users within a specific frequency bandwidth cannot exceed the defined limit [1,2,3,4,5].

Furthermore, co-channel interference escalates proportionally with the augmentation of user count. Following the advancement of highdefinition video (HD) resolution and quadruple high definition (QHD), handheld devices faced challenges transmitting or receiving large-sized videos over 3G and 4G frequency channels. Therefore, having a broader frequency range and quicker data transfer speeds is imperative for the efficient transmission and wireless reception of high-quality multimedia content between two terminals. To address this issue, the frequencies of 5G are being carefully examined due to their broader bandwidth. 5G has a wider bandwidth and a more significant number of frequency channels than 3G and 4G, making it suited for a growing number of customers requiring rapid data speeds while on the move.

Recently [6,7,8]. There has been a push for implementing 5G technology in Indonesia. 5G technology represents a new generation of radio systems with a network design that offers highspeed connectivity, strong reliability, little delay, and the ability to support many devices for both the community and the Internet of Things. The user's text is "[2]." 5G technology utilizes highfrequency domains with tiny wavelengths, specifically those covered by Millimeter Wave (mm Wave) [9,10]. Millimeter-wave frequency refers to a high-frequency band between 3 GHz and 300 GHz. It is commonly employed in millimeter-wave technology for short-distance communication and can also serve as a backbone in communication network systems. The most suitable frequency ranges in Indonesia are 700 MHz, 3.5 GHz, 26 GHz, and 28 GHz [4]. The table below provides a comprehensive overview of the several candidates within the world's 5G frequency range [11-13]

The advancement of mobile communication technology has significantly impacted people's lives worldwide. The advent of wireless communication networks has significantly transformed human communication, idea

sharing, and lifestyle over the past decade. Both utilize third-generation (3G) and fourthgeneration (4G) cellular networks. The world is gearing up to implement the fifth generation (5G). This versatile platform can seamlessly combine diverse wireless communication technologies and services while also offering ubiquitous connectivity. According to Vigilante [14] [15], t5G technology would surpass past technologies and generate a concept known. This refers to a connected environment that can encompass everything in our surroundings. Antennas play a crucial role in cellular telecommunication systems. High frequencies can reduce antenna size, requiring an easily integrated 5G technology-compatible antenna. Microstrip antennas are a viable candidate for 5G technology. Microstrip antennas have the characteristics: being following slender. compact, readily integrable, and capable of functioning at high frequencies. Microstrip antennas have a drawback, specifically a limited bandwidth [8], necessitating the implementation of specialized approaches to enhance their bandwidth. Furthermore, microstrip antennas necessitating have minimal gain, preparation techniques. An array configuration can improve an antenna's amplification and sensitivity [8], producing a more focused antenna beam directionality. This is essential in 5G technologies [16,17,18]. In 2019, Fajar Wahyu Adriano and his team conducted a study on the design of a microstrip antenna. Fajar Wahyu radiant and his team designed the antenna with a rectangular patch shape and added a U-slot to enhance its bandwidth. The antenna was designed to operate at a 28 GHz frequency and was arranged in a 1×2 array to increase its gain. Furthermore, engineered the antenna demonstrates a focused radiation pattern in one direction and aligns its polarization straightly. 5G technology uses antennas for communication. This study aims to develop and evaluate the performance of a rectangular 1x2 array microstrip antenna operating at a frequency of 3.5 GHz. The researchers anticipate that the voltage standing wave ratio (VSWR) parameter test will yield results of < 2, and the return loss parameters will be \leq -10 dB.

2. ANTENNA MODELS AND COMPUTATIONAL METHODS

The radiation patterns of the active arrays have been determined by utilizing the cavity model for the rectangular patch, the simple Green's function model, and the IE3D electromagnetic simulator from Zeland Software, Inc. It was assumed that the ground plane is unlimited for all three scenarios. The calculations did not incorporate the parameters of the Gunn diodes. The characteristics of the Gunn diode primarily affect the resonant frequency or the input impedance matching. However, their impact on the co-polarization radiation patterns is expected to be insignificant. Furthermore, the effect of the DC bias line was disregarded [19,20].

2.1. Simple Green's function model

The spectral domain refers to the range of frequencies or wavelengths present in a signal or phenomenon. The electric field on the patch has been computed using Green's function for the grounded dielectric slab. The assumption of a cosine current distribution on the patch obviated the necessity of calculating the patch currents utilizing the method of moments. The far field is determined by applying the equivalence principle, which states that the far field is directly related to the Fourier transformation of the electric field at the highest dielectric boundary. The Green's function is computed using the numerical algorithm G1DMULT [21,22].

3. ANTENNA ARRAYS

3.1 Modified patch antenna

This study utilized a modified rectangular patch antenna with a Gunn diode integrated into a rectangular aperture to address issues caused by disruption in the current patch distribution. The active element cap size became significant about the wavelength, making it difficult to establish adequate impedance matching. By incorporating an active single-port signal into a rectangular

patch aperture, the antenna's feed point, and input impedance were more precisely determined, leading to enhanced oscillator performance [23]

The rectangular microstrip patch had dimensions of 10.2 mm x 15.3 mm and a rectangular aperture measuring 4 mm x 5 mm. The overlay was applied onto a substrate with a thickness of 0.54 mm and a relative permittivity (er) of 2.18. Both modified rectangular pads were equipped with 50mW Gunn Diodes (MA49106) tightly packed. The Gunn diode's DC bias was established using a high-impedance microstrip wire connected to the non-radiating edge of the patch near its center [23]. Frequency tuning was achieved by altering the direct current (DC) bias voltage applied to the Gunn diode. The presence of a rectangular hole resulted in a decrease in the resonant frequency of the patch and a reduction in the quality factor of the patch resonator. The Gunn diode achieved an appropriate impedance match to generate oscillations at a frequency slightly higher than the resonance frequency of the patch [..]. Two altered patches were included in active arrays linked in the E plane and H plane. To achieve simultaneous injection coordination, the active patches' oscillation frequencies were regulated by adjusting their DC bias voltage. Each active antenna has a tuning range of approximately 300 MHz, but due to manufacturing tolerances of the Gunn diode, the injection is mutually blocked by 200 MHz. The highest attainable scanning angle is defined by the spacing between elements in the array and the range within which phase locking is possible. [24,25].

3.2 E plane array

The two active oscillating antennas were coupled in the E plane and placed 0.63 λ apart (Fig. 1). The active patch orientation in the array introduced an additional phase shift of 180° between the signals radiated by the two patches. Radiation coupling was strong enough to

ensure the stable operation of the array. The operating frequency was 9.68 GHz. By changing the DC bias voltage of one of the active

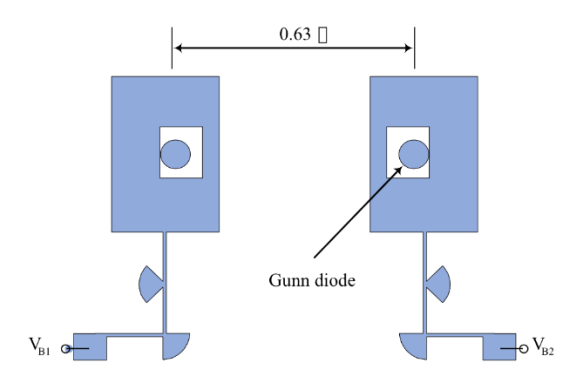


Fig 1. E Plane Active Patch Array

Achieved is a symmetrical beam scanning of ±20° around the broadside by applying patches. Due to the little imbalance of the primary beam in both the directed scenarios. the position of the primary beam was not decided by the direction of the highest intensity but rather as the point that is symmetrical to the beam's 3 dB points. The center of the beam is 1 dB below the maximum level. The cross-polarization values observed across the scanning range in the main beam direction were below -20 dB. The E plane array's EIRP (Effective Isotropic Radiated Power) was around 700 milliwatts. An efficiency of 109% has been achieved for broadside radiation combining, while for the steered situations. the efficiency approximately 84%. The phenomenon of achieving a combining efficiency of over 100% can be attributed to the improved impedance matching when the active antennas are combined into an array using Gunn diodes. When steering is employed, the effectiveness of combining falls due to power being emitted through the side lobes. This occurs because the inter-element spacing inside the array is more excellent than half the wavelength, leading to the high side lobes. Figures 2, 3, and 4 compare measured and

estimated radiation patterns for broadside radiation, -20°, and +20° directed instances. The models and procedures outlined in section 2 were used to calculate the results. The figures show that the co-polarization radiation patterns exhibit a firm agreement with the data. The primary beam and null positions are accurately forecasted. However, none of the techniques anticipated the asymmetry of the primary beam. This asymmetry can be attributed to the limited and relatively small ground plane and heat sink in the actual scenario. [26]. As anticipated, the calculated cross-polarization values in the E plane are shallow and are not depicted in Figure 2.

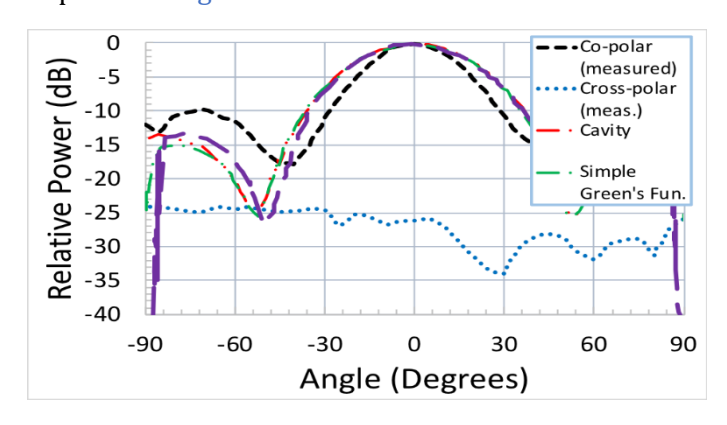
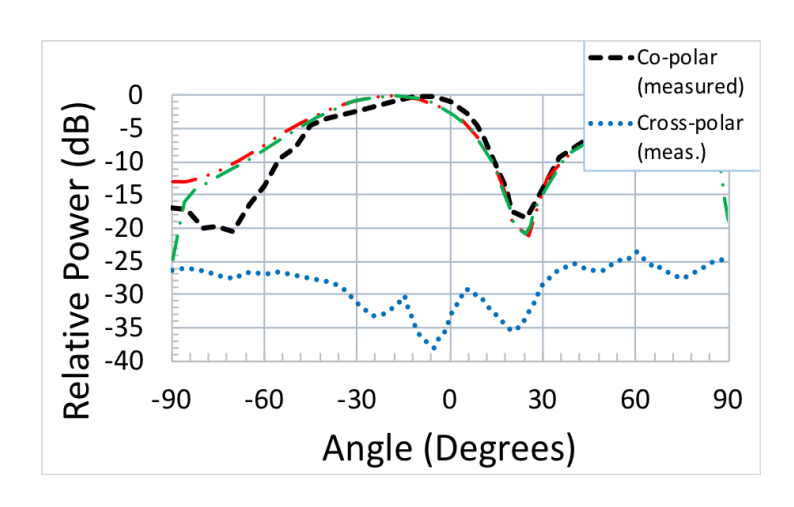
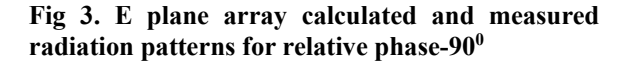


Fig 2. E plane array calculated and measured radiation patterns for broadside radiation





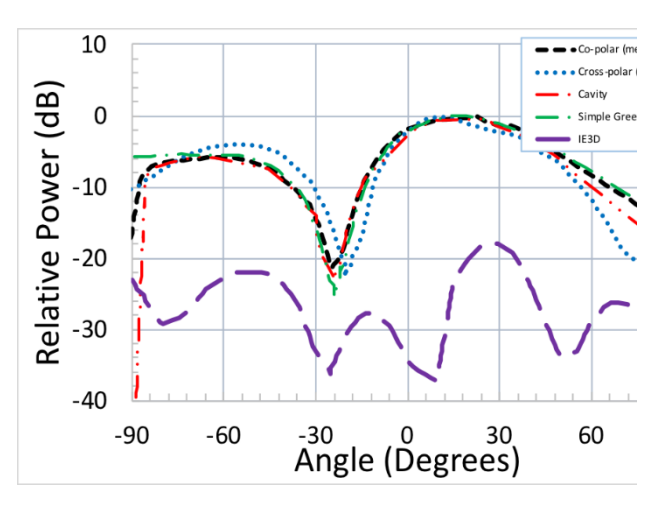


Fig 4. E plane array calculated and measured radiation patterns for relative phase +90°

3.3 H plane array

The study utilized a modified rectangular patch antenna with a Gunn diode integrated into a rectangular aperture to address issues caused by a disruption in the current patch distribution. The active element cap size became significant regarding wavelength, making it difficult to establish adequate impedance matching. By incorporating an active single-port signal into a rectangular patch aperture, the antenna's feed point and input impedance were more precisely determined, leading to enhanced oscillator The modified performance. patch dimensions of 10.2 mm x 15.3 mm and a rectangular aperture of 4 mm x 5 mm. The antenna was applied onto a substrate with a thickness of 0.54 mm and a relative permittivity of 2.18. The Gunn diode's DC bias was established using a high-impedance microstrip wire connected to the non-radiating edge of the patch near its center. Frequency tuning was achieved by altering the direct current bias voltage applied to the Gunn diode. Two altered patches were included in active arrays linked in the E and H planes, regulating the oscillation frequencies of the active patches.

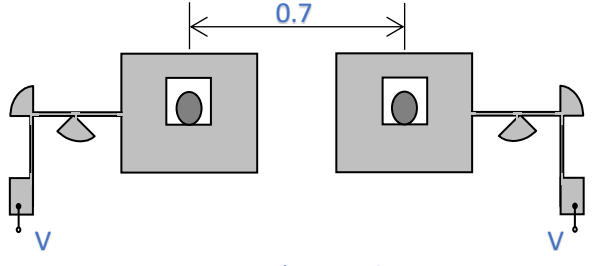


Fig. 5. H plane active

The impact of a thin dielectric slab on the array's operating mode has been observed. A summation pattern was observed when the slab was positioned at 24.9 mm, while a distinct pattern with a null point at the broadside was achieved when the slab was positioned at 17.3 mm. Beam scanning was accomplished for both positions of the dielectric slab. The cavity model accurately predicted the position of the main beam, but side lobes were moved towards more considerable angles. Green's function model and IE3D simulator considered the impact of the dielectric slab on radiation patterns. The G1DMULT numerical approach in the simple Green's function model efficiently computed Green's function considering the presence of a thin dielectric slab in front of the array. However, the calculated side lobe values were lower than the observed ones. This can be explained by the hypothetical scenario where a portion of the emitted energy becomes confined within the parallel plate waveguide formed by the infinite ground plane and the dielectric slab positioned in front of the array. The cross-polarization levels estimated using IE3D accurately predicted the observed behavior of the cross-polarization levels but were consistently 5 to 10 dB lower than the measured values [27,28,29].

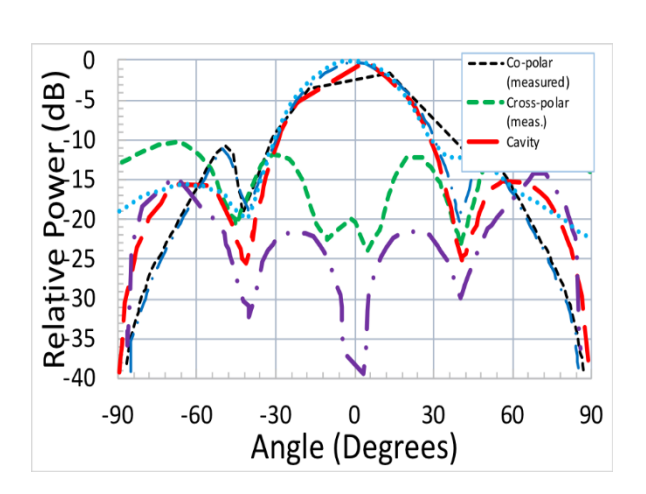


Fig 6. H plane array calculated and measured radiation patterns for broadside radiation

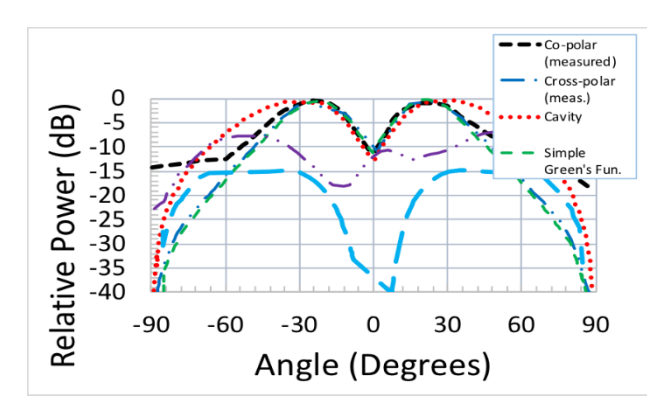


Fig 7 H plane array calculated and measured difference radiation patterns for broadside radiation.

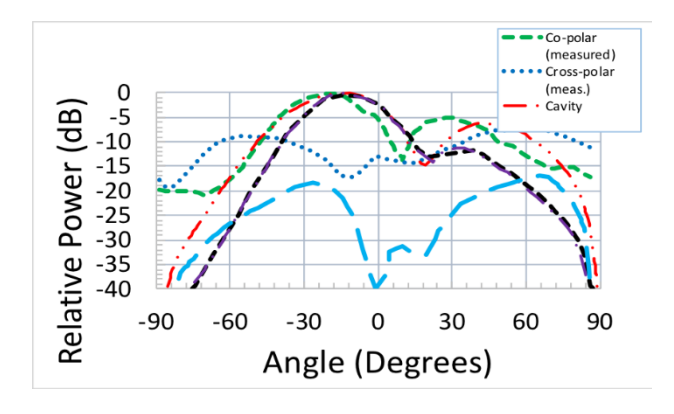


Fig 8. H plane array calculated and measured radiation patterns for relative phase +90°

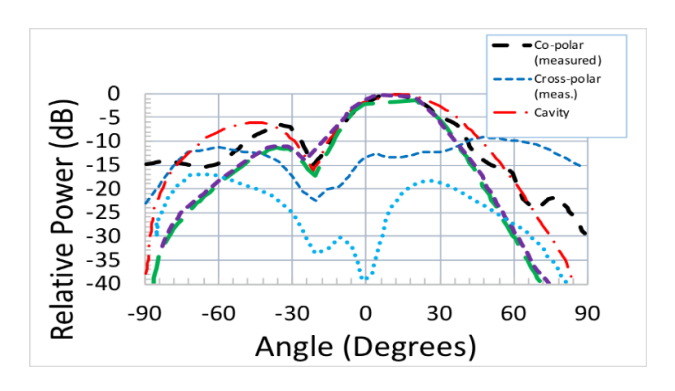


Fig 8. H plane array calculated and measured radiation patterns for relative phase - -900

4. Conclusions

Three simulation models were used to calculate the radiation patterns of two-element active patch arrays coupled in the E and H planes. The radiation coupling was strong enough for the active array in E plane to assure stable operation. The power combining efficiency varied from its maximal value for broadside radiation to minimal values for the two steered cases. In the steered instances a significant amount of the energy is radiated through the side lobes which are pretty high because of the array inter-element spacing larger than half wavelength. Symmetrical beam scanning around the broadside was obtained. All three models predicted the main beam position and radiation pattern null location very well. The calculated beam width for broadside radiation is slightly larger than the measured one.

A thin dielectric slab was used to increase the mutual coupling between the active antennas in the H-plane array to achieve stable operation. With the same DC bias on the active elements, the array operated in even or odd mode, depending on the dielectric slab position in front of the variety. The asymmetrical beam scanning around the broadside, in this case, can be attributed to the difference in the powers radiated by the two active antennas in the array. The simple Green's function model and IE3D simulator accurately predicted the main beam shape and radiation pattern null positions. The cavity model gave less accurate but rather satisfactory results, considering its simplicity. For both arrays, the discrepancy between calculated and measured radiation patterns increases when approaching ±90°. This is due to the infinite ground plane assumption in all models used for calculation.

5. References

[1] Roshani, S. & Shahv, H., 2021. Mutual Coupling Reduction In Microstrip Patch Antenna Arrays Using Simple Microstrip Resonator. Available at: http://dx.doi.org/10.21203/rs.3.rs-456147/v1.

[2] Cock, R. & Christodoulou, C., Design of a twolayer, capacitively coupled, microstrip patch antenna element for broadband applications. 1987 Antennas and Propagation Society International Symposium. Available

http://dx.doi.org/10.1109/aps.1987.1149998.

- [3] Mujawar, M., 2021. Compact Microstrip Patch Antenna Design with Three I-, Two L-, One E- and One F-Shaped Patch for Wireless Applications. Microstrip Antenna Design for Wireless Applications, pp.57–68. Available at: http://dx.doi.org/10.1201/9781003093558-7.
- [4] Anon, 2015. Microstrip Patch Antenna. Fundamentals of Aperture Antennas and Arrays, pp.137–147. Available at: http://dx.doi.org/10.1002/9781119127451.ch5.
- [6] Fang, Y. And Zhang, Y., 2022. Theory and Experiment on Stacked Circular Microstrip Patch Antennas for Low-Coupling Array Design. IEEE Antennas and Wireless Propagation Letters.
- [7] Mandal, S. and Ghosh, C.K., 2022. Mutual coupling reduction in a patch antenna array based on planar frequency selective surface structure. Radio Science, 57(2), p.e2021RS007392.
- [8] Muraleedharan, M. and Menon, S.K., 2019, April. Isolation Enhancement of Two Element Array using Microstrip Resonator. In 2019 3rd International Conference on Trends in Electronics and Informatics (ICOEI) (pp. 1042-1046). IEEE.
- [9] Al Smadi Takialddin, K.A.S. and Orayb, O., AL-Smadi, High-Speed for Data Transmission in GSM Networks Based on Cognitive Radio. American Journal of Engineering and Applied Sciences, 10(1), pp.69-77.
- [10] C. Varadhan, J. K. Pakkathillam, M. Kanagasabai, R. Sivasamy, R. Natarajan and S. K. Palaniswamy, "Triband Antenna Structures for RFID Systems Deploying Fractal Geometry," IEEE Antennas and Wireless Propagation Letters, vol. 12, pp. 437-440, 2013.
- [11] O. Ouazzani, S. D. Bennani and M. Jorio, "Design and Simulation of 2*1 and 4*1 Array Antenna for Detection System of Objects or Living Things in motion", International Conference on

- Wireless Technologies Embedded and Intelligent Systems WITS-2017.
- [12] Al-Sawalha, A. and Al Smadi, T., 2018. Microstrip Patch Antenna Radiation Variation of Quality Factors and Bandwidth of a Conically Depressed. Journal of Advanced Sciences and Engineering Technologies, 1(1), p.7.
- [12] Alkhawaldeh, I. and Al Smadi, T., 2022. Micro-Strip Antenna Array for Telecommunication Systems. European Journal of Applied Sciences–Vol, 10(2).

- [13] Al-Sawalha, A. and Al Smadi, T., 2018. Engineering Technology microstrip patch antenna radiation Variation of Quality Factors and Bandwidth of a Conically Depressed. Journal of Advanced Sciences and Engineering Technologies, 1(1), pp.1-6. [14] Al Smadi, T. A. (2011). Low cost smart sensor design. Am. J. Eng. Applied Sci, 4, 162-168.
- [15] Mohanty, M. N., Satrusallya, S., & Al Smadi, T. (2022). Antenna selection criteria and parameters for IoT application. In Printed Antennas (pp. 283-295). CRC Press.
- [16] Al-Sawalha, A., & Al Smadi, T. (2018). Microstrip Patch Antenna Radiation Variation of Quality Factors and Bandwidth of a Conically Depressed. Journal of Advanced Sciences and Engineering Technologies, 1(1), 7.
- [17] Takialddin, Al Smadi. "Performance Study of Broadband and a Dual-Band Antenna-Array of Telecommunication Systems." Anbar Journal of Engineering Sciences 13, no. 2 (2022): 74-83.
- [18] Al Smadi, T., & Al-Taweel, F. M. (2022). Microstrip patch Antenna Array for Wireless Design Applications. Journal of Advanced Sciences and Engineering Technologies, 5(1), 66-75.
- [19] Al-Sawalha, A., & Al Smadi, T. (2018). Engineering Technology microstrip patch antenna radiation Variation of Quality Factors and Bandwidth of a Conically Depressed. Journal of Advanced Sciences and Engineering Technologies, 1(1), 1-6.
- [20] Takialddin, A. S., Al Smadi, K., & AL-Smadi, O. O. (2017). High-Speed for Data Transmission in GSM Networks Based on Cognitive Radio. American Journal of Engineering and Applied Sciences, 10(1), 69-77.
- [21 Takialddin, A. S. (2024). Review of the optimization Machine Learning Inverse of view—Mode Fiber and. Journal of Advanced Sciences and Engineering Technologies, 7(1), 22-35.
- [22] Trrad, Issam, T. A. Smadi, and Hassan Al_Wahshat. "Application of fuzzy logic to cognitive wireless communications." International Journal of Recent Technology and Engineering (IJRTE) 8, no. 3 (2019): 2228-2234.
- [23] Al-Aziz, A., Myaser, K., Hamood, M. A., Najam, L. A., Al–Sawalha, A., & Ahmed, H. M. (2023). Shielding Properties of Al-Cu-Pb Alloys by XCOM and Experimental Data. Rafidain Journal of Science, 32(2), 31-38.
- [24] Najam, L. A., & Al Sawalha, A. (2021). Adaptive anti-synchronization of nuclear spin generator (NSG) systems with fully uncertain parameters. Journal of Advanced Sciences and Engineering Technologies, 4(1), 16-24.
- [25] Smadi, T.A. and Al-Sawalha, A., Variation of Quality Factors and Bandwidth of a Conically

Depressed Microstrip Patch Antenna in Plasma Medium.

[26] Hussein, A.L., Trad, E. and Al Smadi, T., 2018. Proactive algorithm dynamic mobile structure of Routing protocols of ad hoc networks. IJCSNS, 18(10), p.86.

Appleton–Hartree magnetoionic theory. Canadian Journal of Physics, 90(3), 241-247.

[27] Bai, Y.Y., Xiao, S., Liu, C., Shuai, X. and Wang, B.Z., 2013. Design of pattern reconfigurable antennas based on a two—element dipole array model. IEEE Transactions on Antennas and Propagation, 61(9), pp.4867-4871.

[28] Apostolov, Peter. "Efficient Two-Element Array Antenna." In 2021 12th National Conference with International Participation (ELECTRONICA), pp. 1-4. IEEE, 2021.

[29] Bawa'aneh, M. S., Al-Khateeb, A. M., & Sawalha, A. S. (2012). Microwave propagation in a magnetized inhomogeneous plasma slab using the